J Mater Sci (2013) 48:2690–2700
DOI 10.1007/s10853-012-7064-0

Preparation and properties of nanofiber-coated composite membranes as battery separators via electrospinning

Mataz Alcoutlabi · Hun Lee · Jill V. Watson · Xiangwu Zhang

Received: 29 October 2012 / Accepted: 1 December 2012 / Published online: 11 December 2012

Abstract An electrospun nanofiber-coated Celgard® 2400 polypropylene microporous battery separator was prepared using polyvinylidene fluoride (PVDF) and polyvinylidene fluoride-*co*-chlorotrifluoroethylene (PVDF-*co*-CTFE). The coating of PVDF and PVDF-*co*-CTFE nanofibers was carried out using single nozzle and nozzle-less electrospinning methods. The nanofiber coating prepared by the nozzle-less electrospinning method was found to have better adhesion to the microporous separator membrane than the nanofiber coating prepared by single nozzle electrospinning. The PVDF and PVDF-*co*-CTFE nanofiber coatings increased the electrolyte uptake capacity in a secondary lithium-ion battery, with PVDF-*co*-CTFE co-polymer nanofiber-coated microporous membrane showing higher electrolyte uptake capacity than PVDF homopolymer-coated microporous membrane. In addition, the PVDF and PVDF-*co*-CTFE nanofiber coatings improved the adhesion of the porous microporous membrane to a battery electrode. It was also found that nanofiber coatings prepared by the nozzle-less electrospinning method have better adhesion properties and higher electrolyte uptake capacity than those by single nozzle electrospinning.

Mataz Alcoutlabi and Hun Lee contributed equally to this work.

M. Alcoutlabi · H. Lee · X. Zhang (✉)
Fiber and Polymer Science Program, Department of Textile Engineering, Chemistry and Science, North Carolina State University, Raleigh, NC 27695-8301, USA
e-mail: xiangwu_zhang@ncsu.edu

J. V. Watson
Celgard LLC, 13800 South Lakes Drive, Charlotte, NC 28273, USA

Introduction

Lithium-ion batteries are widely used as a power source for portable electronic devices and hybrid electric vehicles due to their excellent energy and power densities, long cycle life, and enhanced safety [1–5]. A critical component of lithium-ion batteries is the microporous separator which is placed between the positive and negative electrodes of the battery. The main function of the separator is to prevent the physical contact of electrodes while serving as the electrolyte reservoir to enable ionic transport.

Polyolefin microporous membranes are commonly used as separators for lithium-ion batteries due to their excellent performance properties, such as good chemical stability and high mechanical strength [4, 6–8]. Recently, researchers have modified polyolefin microporous membranes using different coating methods to improve surface properties of the membrane. Numerous patents have been published on technologies which use a variety of coating methods to deposit functional polymers on the surface of the separator membranes. Common coating methods are dip coating [9–12], laminate [13–15], slot die [16, 17], gravure coating [18, 19], and curtain coating [20, 21]. The coated layer applied by these methods must not compromise the performance properties of the battery and should be designed to enhance both the porous and tortuous structure of the membrane and to improve the battery electrolyte uptake capacity.

In order to address these challenges, several research groups have used electrospinning method to prepare nanofiber-based porous separators with a variety of polymers, such as polyacrylonitrile (PAN) [22–25], polyvinylidene fluoride (PVDF) [26–31], polyvinylidene fluoride-*co*-hexafluoropropylene (PVDF-*co*-HFP) [32–34], and polymethyl methacrylate (PMMA) [35]. These nanofiber membranes

have high porosities, which is beneficial for increasing the electrolyte uptake capacity. Electrolyte uptake capacity is an important property for battery separators, since they have to absorb a significant amount of liquid electrolyte to achieve low internal resistance and sufficient cell performance [36, 37]. In addition, nanofiber separator membranes have improved adhesion to the battery electrodes, which can help prevent the formation of gaps between the separators and electrodes during prolonged charge–discharge cycles, especially in large-format batteries. Even a small failure of the interfacial adhesion between the separator and the electrode can increase battery impedance and cause uneven current distribution leading to the formation of lithium dendrite growth [38]. Many of these nanofiber membranes can provide adhesion to a battery electrode by using polymers such as PVDF and PVDF co-polymers such as PVDF-*co*-HFP. The type of polymer for electrospinning is important as some electrospun nanofiber membranes are typically weak and can be easily damaged during the assembling of lithium-ion batteries [4, 6].

This paper reports the preparation of a composite separators prepared by coating a Celgard® 2400 polypropylene (PP) monolayer microporous membrane separator with PVDF and polyvinylidene fluoride-*co*-chlorotrifluoroethylene (PVDF-*co*-CTFE) nanofibers. PVDF and PVDF-*co*-CTFE were selected due to their excellent electrochemical and thermal stabilities, good adhesion properties, and high mechanical strength. The resultant nanofiber-coated membranes have the potential to combine advantages of both polyolefin separator membrane (e.g., good chemical stability and high mechanical strength) and nanoscale fibrous polymer coating (e.g., high porosity and high surface area). The coating of nanofibers was carried out using single nozzle and nozzle-less (or up-spinning) electrospinning methods. The results of this study show that a coating of PVDF and PVDF-*co*-CTFE nanofibers applied to a PP microporous membrane separator can improve electrolyte uptake capacity and the adhesion of the separator membrane to a battery electrode in a lithium-ion secondary battery. The PVDF polymer type, the electrospinning method, and electrospinning process parameters can impact the structure and properties of the nanofiber-coated microporous battery separator membranes.

Experimental

Materials

Microporous PP separator membrane (Celgard® 2400, Celgard LLC), with a porosity of 41 % and thickness of 25 μm, was used as the base substrate membrane for the deposition of nanofibers. PVDF (Kureha W#9100) and PVDF-*co*-CTFE (Solvay® Solef 32008), both with a molecular weight of 280,000 g/mol, were used for preparing the electrospun nanofiber coatings. The basic properties of these two polymers are summarized in Table 1. Electrospinning solutions (15 wt %) were prepared in a solvent mixture of *N*,*N*-dimethylformamide (DMF) and acetone (7:3 by weight).

Table 1 Molecular structure, monomer, molecular weight, and melting temperature of polymer materials

	Molecular structure	Monomer	Molecular weight (g/mol)	Melting temperature (°C)
PVDF	Homopolymer	$CH_2=CF_2$	280,000	173
PVDF-*co*-CTFE	Co-polymer	$CH_2=CF_2$ and $ClCF=CF_2$	280,000	168

Preparation of nanofiber-coated separator

Nanofiber coatings were prepared by two different electrospinning methods. In the first method, electrospun nanofibers were deposited by using the single nozzle, lab-scale electrospinning device shown in Fig. 1. A high voltage was applied between the electrospinning solution contained in a syringe and the grounded metallic collector. When the voltage reached a critical value, the electrostatic force overcame the surface tension of the pendant drop of the polymer solution at the tip of the nozzle and a liquid jet was ejected. Nanoscale fibers were deposited on surface of the PP separator membrane accumulating and forming a nanofibrous coated layer. Nozzle electrospinning parameters can be easily controlled; however, the production rate of nanofibers is low and the sample size obtained is relatively small (typically, 11–12 cm in diameter).

In the second method, the nozzle-less electrospinning device (NanoSpider™ NS200, Elmarco) shown in Fig. 2 was used. The electrospinning polymer solution was placed in an open bath. To form stable polymer jets, multiple patterned wires were attached to a wire electrode as shown in Fig. 2, and were rotated in bath to be wetted by the electrospinning solution. A high voltage was applied to the solution and multiple jets were ejected from the patterned wire surface in an 'up-spinning' fashion. Dry fibers were deposited onto the PP membrane which was moved continuously at a fixed speed passing over a grounded collector. Compared with the single nozzle-based approach, nozzle-less electrospinning has higher production rate with multiple jets simultaneously generated. In this work, the nozzle-less electrospinning generated a continuous nanofiber coating with a width of 16–17 cm on the Celgard® 2400 PP microporous membrane separator.

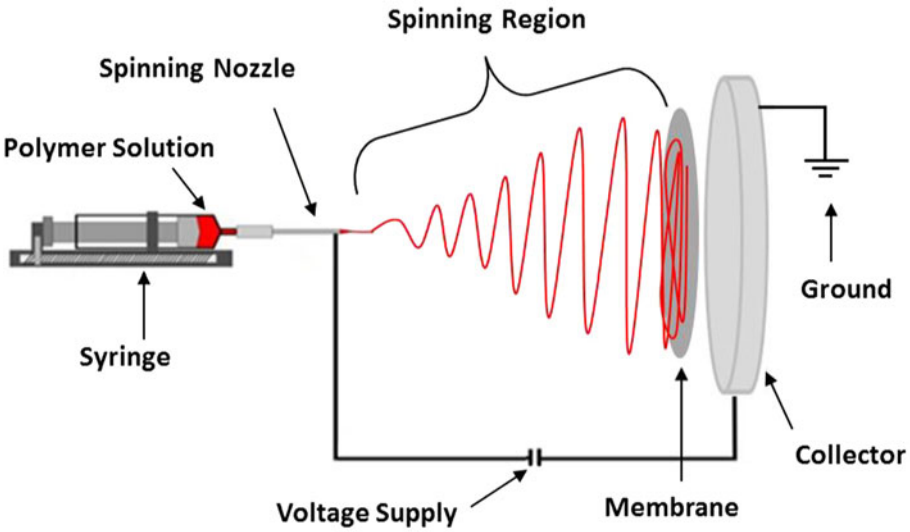

Fig. 1 Schematic of single nozzle electrospinning device

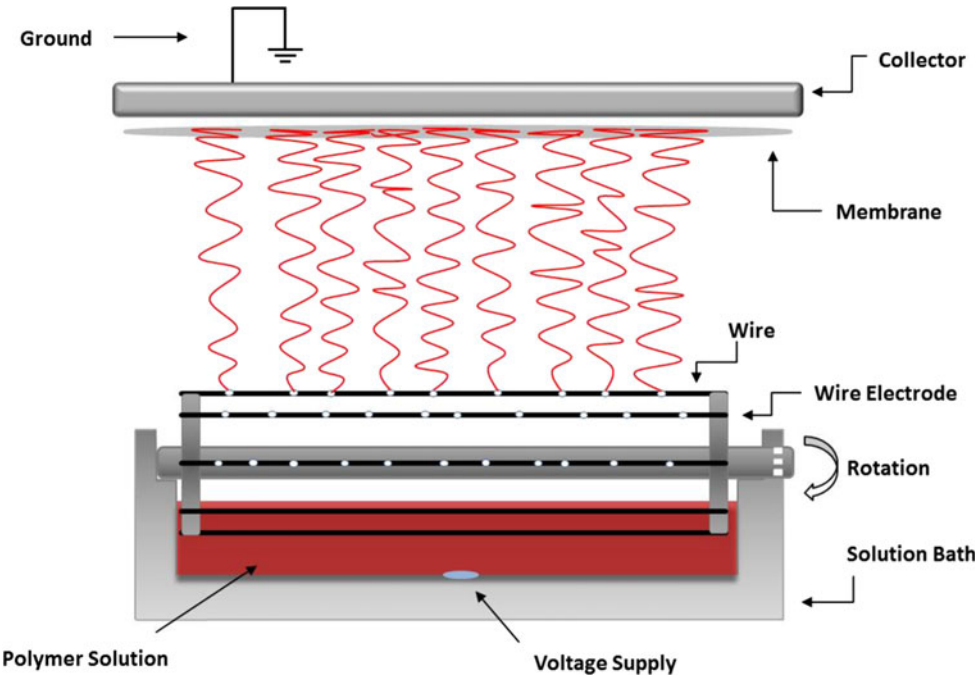

Fig. 2 Schematic of nozzle-less electrospinning device

In both single nozzle and nozzle-less methods, the electrospinning process conditions were controlled so that nanofibers produced had comparable morphology and nanofiber loading (0.9–1.1 g/m^2). The process conditions used for the single nozzle electrospinning of the PVDF polymer were: (1) applied voltage = 15 kV, (2) nozzle-to-collector distance = 25 cm, (3) flow rate = 0.75 ml/h, and (4) deposition time = 3 min, while those for PVDF-*co*-CTFE were: (1) applied voltage = 25 kV, (2) nozzle-to-collector distance = 20 cm, (3) flow rate = 0.25 ml/h, and (4) deposition time = 5 min. For nozzle-less electrospinning, the conditions used for both PVDF and PVDF-*co*-CTFE were: (1) applied voltage = 40 kV, (2) electrode-to-collector distance = 15 cm, (3) electrode rotational speed = 6 r/min, and (4) membrane movement speed = 0.26 m/min.

Structure characterization and property measurements

The morphology of both uncoated and nanofiber-coated PP membranes was evaluated using a scanning electron microscopy (JEOL 6400F Field emission SEM at 5 kV). Samples prepared for SEM analysis were coated with Au/Pd by a K-550X sputter coater to reduce charging. The diameters of electrospun fibers were obtained by measuring

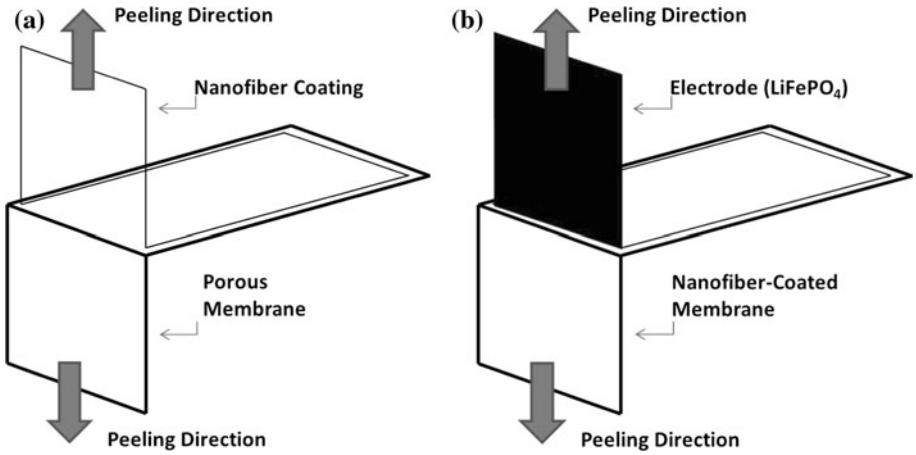

Fig. 3 Schematic of peeling tests for measuring the adhesion between **a** nanofiber coating and PP membrane and **b** nanofiber-coated PP membrane and battery electrode

fifty fibers randomly selected in SEM images using Revolution v1.6.0 software.

Liquid electrolyte uptake capacities were measured by soaking pre-weighed nanofiber-coated separator membrane samples for a fixed time at room temperature in a liquid electrolyte which consisted of 1 M lithium hexafluorophosphate ($LiPF_6$) dissolved in 1:1:1 (by volume) ethylene carbonate/dimethylcarbonate/ethylmethyl carbonate. The electrolyte was absorbed both on the surface and in the pores of the microporous membranes. The excess electrolyte solution adhering to the separator membrane surface was removed by gently wiping with filter paper. The electrolyte uptake capacities of nanofiber-coated separator membranes were determined using the following equation:

$$\text{Uptake Capacity}\left(\text{mg/cm}^2\right) = (W_t - W_0)/A$$

where W_t was the weight of the electrolyte-immersed sample, W_0 the weight of dry sample, and A the immersed area of the test sample.

The adhesion strength of nanofiber coatings to the PP membrane substrate was evaluated by using the ASTM D 1876 standard method, which is a modified ASTM D 2261 standard tongue tear test method using an Instron® Tensile Tester. Figure 3a depicts the modified peel test method used to evaluate the adhesion strength of nanofiber coating layer on the membrane substrate. In this method, the test was carried out on a T-type specimen of two adherends, which were the nanofiber coating and PP membrane, respectively. A test sample measuring 2.5 × 7.5 cm^2 was held in the two jaws of the Instron with the nanofiber coating layer clamped to the movable upper jaw and substrate membrane layer attached to the fixed lower jaw. A tape (3 M Scotch® Magic™ Tape 810) was placed on the backside of the nanofiber coating and the membrane to prevent them from stretching and slippery. The jaws were set at an initial separation distance of 2.5 cm. With the upper jaw moving at a constant rate of 50 mm/min, the nanofiber coating layer was peeled away from the membrane surface at a 90° angle. A 100 N load cell was used for measuring the adhesion strength of the coating through the entire sample length.

The adhesion between the nanofiber-coated membrane and a battery electrode was also evaluated by conducting peel tests on the nanofiber-coated membrane/electrode laminated assemblies, i.e., peeling the electrode away from the nanofiber-coated membrane, as shown in Fig. 3b. The electrode used was a $LiFePO_4$ cathode (MTI Corporation). The nanofiber-coated membrane/electrode assemblies (2.5 × 7.5 cm^2) were prepared by hot pressing the test sample using press plate method (Carver Model C) at 100 °C and 70 psi for 5 min. The peel tests were performed with a 5 N load cell.

The reproducibility of electrolyte uptake capacity and adhesion results was ensured by conducting all measurements on at least eight samples.

Results and discussion

SEM images

Figure 4 shows SEM images of an uncoated Celgard® PP microporous membrane separator. Its morphology presents a microporous structure with uniform distribution of small slit-shaped rectangular pores, ~0.04 μm in diameter. In this work, PVDF and PVDF-*co*-CTFE nanofibers were coated onto the PP microporous membrane separator by using single nozzle and nozzle-less electrospinning methods.

In both single nozzle and nozzle-less electrospinning, there are many process parameters which can influence the formation and morphology of electrospun nanofibers. These parameters include, but are not limited to, solution concentration, applied voltage, nozzle-to-collector distance, solution flow rate, and electrode rotating speed [39–42]. In order to optimize the processing parameters, electrospinning experiments were carried out under various electrospinning

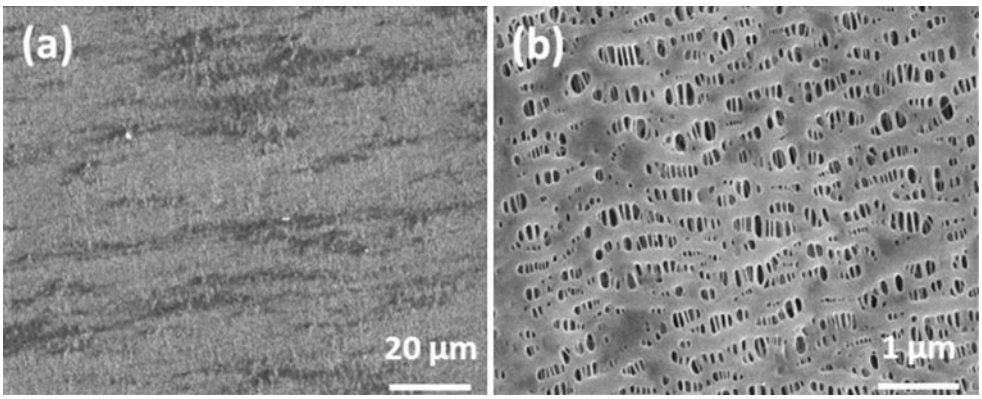

Fig. 4 SEM images of an uncoated PP membrane. Magnification: 1000× (**a**) and 20,000× (**b**)

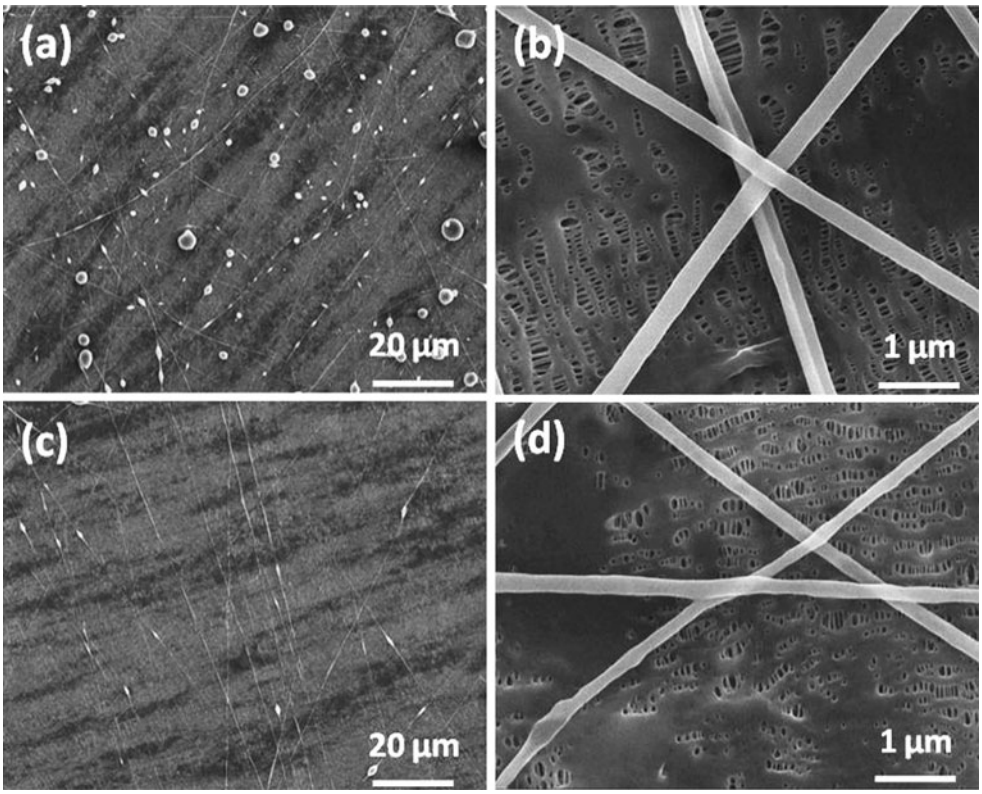

Fig. 5 SEM images of **a**, **b** PVDF and **c**, **d** PVDF-*co*-CTFE nanofiber-coated PP membranes prepared by single nozzle electrospinning. Magnification: 1000× (**a**, **c**), 20,000× (**b**, **d**)

conditions to obtain nanofiber coatings with uniform fiber diameters and well-defined morphology. The optimized electrospinning conditions are shown in the experimental section, and nanofiber-coated PP membranes reported here were prepared based on these conditions. The processing conditions were carefully controlled so that the nanofiber coatings deposited on membrane substrates were produced with comparable thicknesses of 3–4 μm.

Figure 5 shows SEM images of PVDF and PVDF-*co*-CTFE nanofiber-coated PP membranes produced by the single nozzle electrospinning method. The electrospun nanofibers form a random fiber orientation and are adequately interconnected on the surface of the PP membrane to form a fibrous network. Figure 6 shows PVDF and PVDF-*co*-CTFE nanofiber-coated PP membranes produced by the nozzle-less electrospinning method. The electrospun nanofibers prepared by this method also show a randomly oriented and interconnected morphology.

Figure 7 shows average nanofiber diameters PVDF and PVDF-*co*-CTFE nanofiber-coated PP membranes produced by the single nozzle and nozzle-less electrospinning methods. The average fiber diameter produced by single

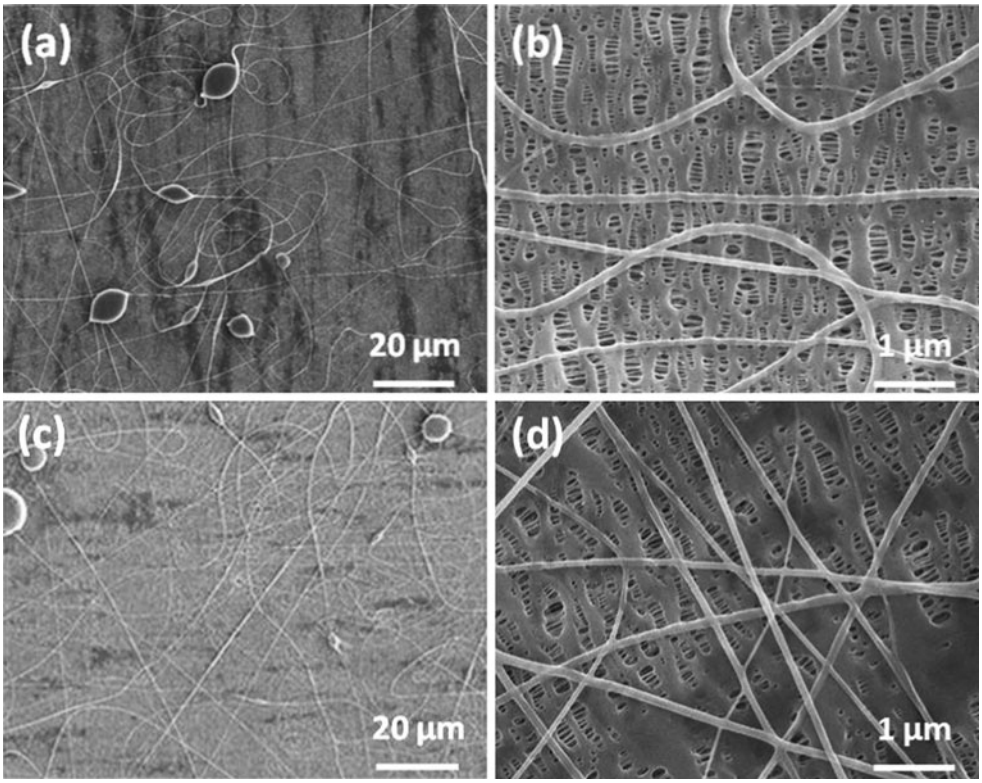

Fig. 6 SEM images of **a**, **b** PVDF and **c**, **d** PVDF-*co*-CTFE nanofiber-coated membranes prepared by nozzle-less electrospinning. Magnification: 1000× (**a**, **c**), 20,000× (**b**, **d**)

nozzle electrospinning is 198 nm for PVDF nanofibers and 186 nm for PVDF-*co*-CTFE nanofibers. However, in the case of nozzle-less electrospinning, average fiber diameter is 138 nm for PVDF nanofibers and 129 nm for PVDF-*co*-CTFE nanofibers. Therefore, nanofibers deposited by nozzle-less electrospinning have smaller diameters than those by single nozzle electrospinning. The smaller diameters may be attributed to the higher voltage used in nozzle-less electrospinning (40 kV), as compared to that in nozzle electrospinning (15 or 25 kV). Higher voltage leads to greater electrostatic force, which is more effective in stretching the spinning jet and is beneficial for forming thinner diameter nanofibers. In addition, due to the use of polar co-monomer ($ClCF{=}CF_2$), PVDF-*co*-CTFE has higher conductivity than PVDF homopolymer and is more sensitive to the electric force, especially in the high voltage nozzle-less electrospinning [41, 43]. In both cases of electrospinning, the high polarity factor of the co-monomer contributed to PVDF-*co*-CTFE nanofibers having smaller fiber diameters than PVDF homopolymer nanofibers.

Adhesion between nanofiber coating and membrane substrate

The PVDF homopolymer and PVDF-*co*-CTFE co-polymer nanofiber-coated PP membrane separators were found to adhere to the PP microporous membrane substrate. Peel tests were carried out to examine the adhesion peel force between the nanofiber coating and the PP membrane substrate. Figure 8a compares the peeling loads of PVDF homopolymer nanofiber coatings prepared by single nozzle and nozzle-less electrospinning. The PVDF nanofiber coatings formed by the nozzle-less electrospinning were found to have greater adhesion to the PP membrane than those prepared by single nozzle electrospinning. In Fig. 8b, nozzle-less electrospinning method also produced PVDF-*co*-CFTE nanofibers with higher adhesion than single nozzle electrospinning.

The adhesion of nanofiber coatings to the PP membrane substrate depends on the nanofiber formation process during electrospinning. In single nozzle electrospinning, the polymer solution is contained in a syringe and evaporation of the solvent occurs after the jet is ejected from the nozzle tip. Since only one jet is present, the amount of evaporated solvent is low within the spinning region while the rate of solvent evaporation from the spinning jet is high. Hence, the fibers deposited on the membrane surface are relatively dry and poorly stick to the PP membrane substrate. In nozzle-less electrospinning, multiple jets are generated simultaneously, while the spinning solution in the liquid bath is exposed to the spinning environment, and as a result, a larger amount of solvent vapor is present. This causes a slower evaporation of solvent from the spinning jets and slower drying of the

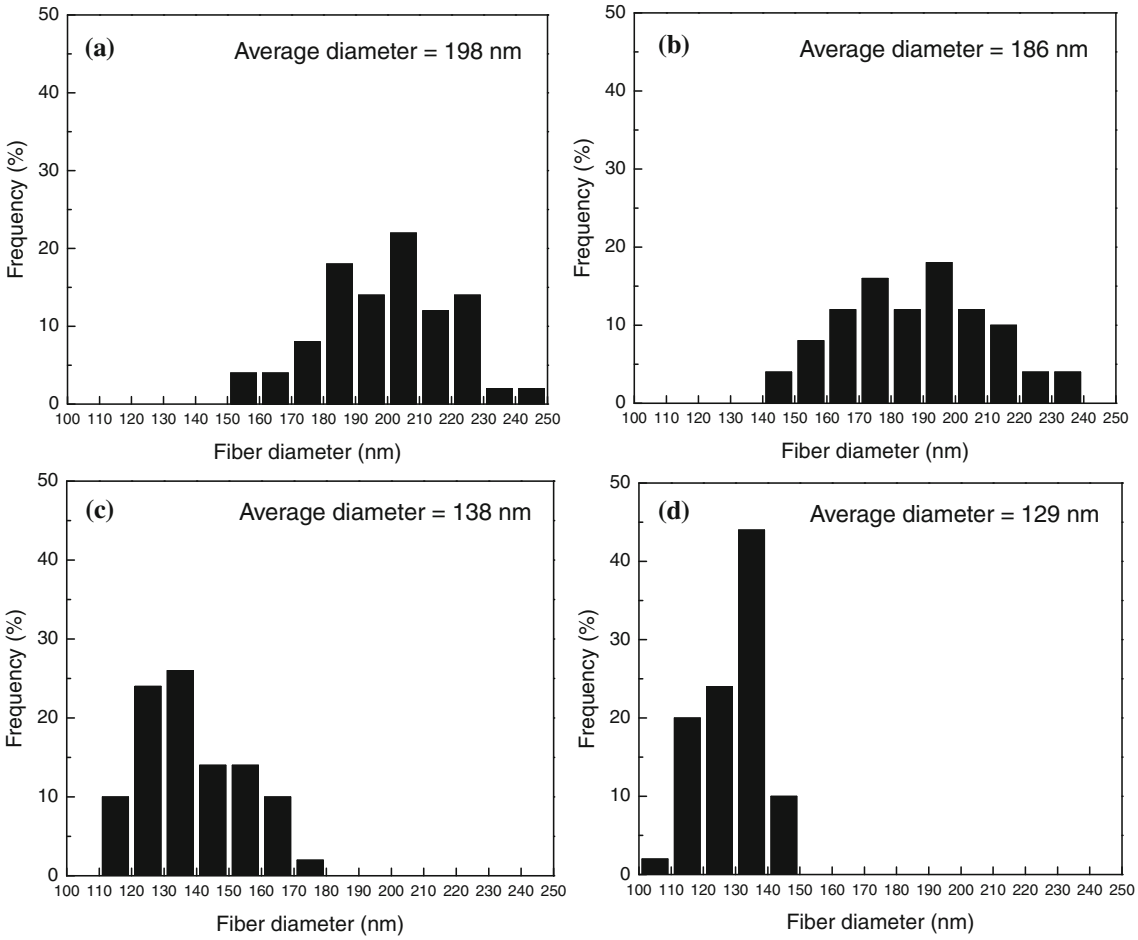

Fig. 7 Fiber diameter distributions of **a** PVDF by single nozzle electrospinning, **b** PVDF-*co*-CTFE by single nozzle electrospinning, **c** PVDF by nozzle-less electrospinning, and **d** PVDF-*co*-CTFE by nozzle-less electrospinning

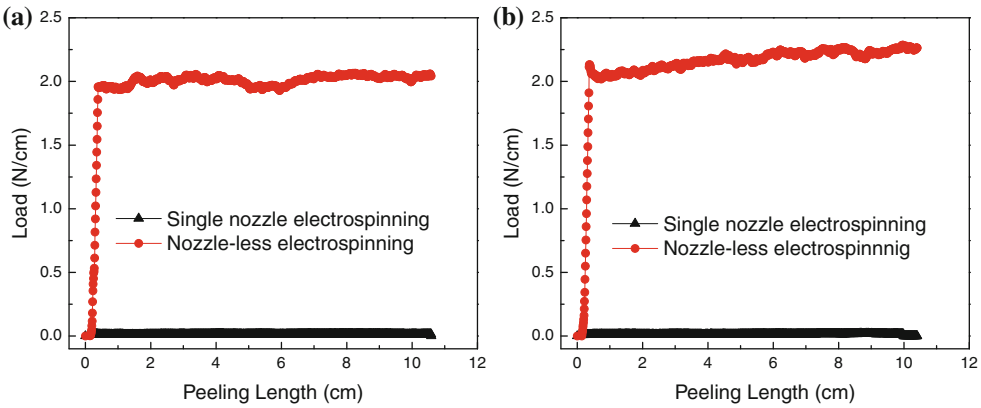

Fig. 8 Peeling load as a function of length for peeling **a** PVDF and **b** PVDF-*co*-CTFE nanofiber coatings from the PP membrane

nanofibers formed. The nanofibers may contain some residual solvent which helps the adhesion of the fibers to the substrate. In addition, the higher voltage in nozzle-less electrospinning leads to a higher flying speed of the spinning jets and a shorter time for the solvent to evaporate before reaching the membrane substrate. Therefore, when the fiber jets arrive at the membrane surface, they have more residual solvent, which results in the formation of nanofibers with improved adhesion to the membrane. Furthermore, nanofibers prepared by nozzle-less electrospinning have smaller fiber diameters than those prepared by single nozzle electrospinning, and thus they have larger contact area with the membrane substrate, which may also contribute to the better adhesion of these nanofibers to the membrane substrate.

Electrolyte uptakes of nanofiber-coated membranes

Electrolyte uptake capacity is an indication on how much battery electrolyte solution can be absorbed by the unit area of a separator membrane. For lithium-ion batteries, the separator should be able to absorb a significant amount of liquid electrolyte in order to achieve a low internal resistance and sufficient cell performance [4, 44]. Figure 9 shows the electrolyte uptake capacities of PVDF and PVDF-*co*-CTFE nanofiber-coated Celgard® PP microporous membranes prepared by single nozzle electrospinning and nozzle-less electrospinning, respectively. For comparison, the electrolyte uptake capacities of uncoated PP microporous membrane are also shown. The electrolyte uptakes increase quickly for all membranes and less than 60 s is required for saturated absorption of liquid electrolyte in separators. Rapid absorption of electrolyte is desirable in the lithium-ion battery assembly process. As shown in Fig. 9, the PVDF and PVDF-*co*-CTFE nanofiber coating layers increases the electrolyte uptake capacities. Due to the presence of polar groups, PVDF and PVDF-*co*-CTFE can absorb liquid electrolyte to form polymer gels [32, 33, 45] contributing to increased electrolyte uptake capacity. When prepared by nozzle-less electrospinning method, the electrolyte uptake capacities of both PVDF and PVDF-*co*-CTFE nanofiber-coated membranes are significantly higher than those of uncoated membranes.

In the case of single nozzle electrospinning, PVDF and PVDF-*co*-CTFE nanofiber-coated membranes have comparable electrolyte uptake capacities due to their similar morphology (Fig. 5). On the other hand, PVDF-*co*-CTFE nanofiber-coated membranes prepared by nozzle-less electrospinning have higher electrolyte uptake capacities compared with PVDF homopolymer nanofiber-coated membranes. The difference in electrolyte uptake capacities is attributed to PVDF-*co*-CTFE nanofibers with smaller fiber diameter than PVDF homopolymer nanofibers.

Adhesion of nanofiber-coated membrane on the electrode

Good adhesion between the separator membrane and the battery electrode is desired for high-performance lithium-ion batteries. Nanofiber-coated separator membrane/electrode assemblies were prepared by hot-pressing a nanofiber-coated membrane onto a battery $LiFePO_4$ cathode using the plate press method at 100 °C and 70 psi. The adhesion between nanofiber-coated membrane and the battery electrode was evaluated by conducting peel tests. Figure 10 shows the peel test results for removing PVDF

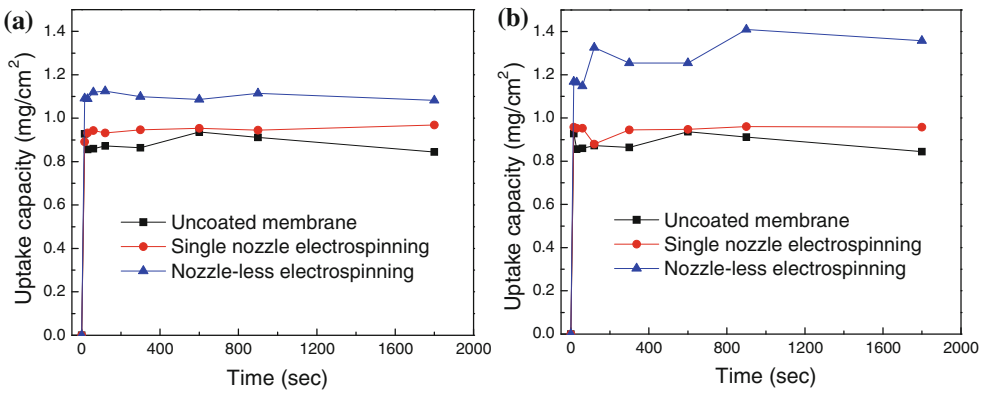

Fig. 9 Electrolyte uptake capacity as a function of time for **a** PVDF and **b** PVDF-*co*-CTFE nanofiber-coated PP membranes prepared by single nozzle electrospinning and nozzle-less electrospinning. For comparison, uncoated membrane is also shown

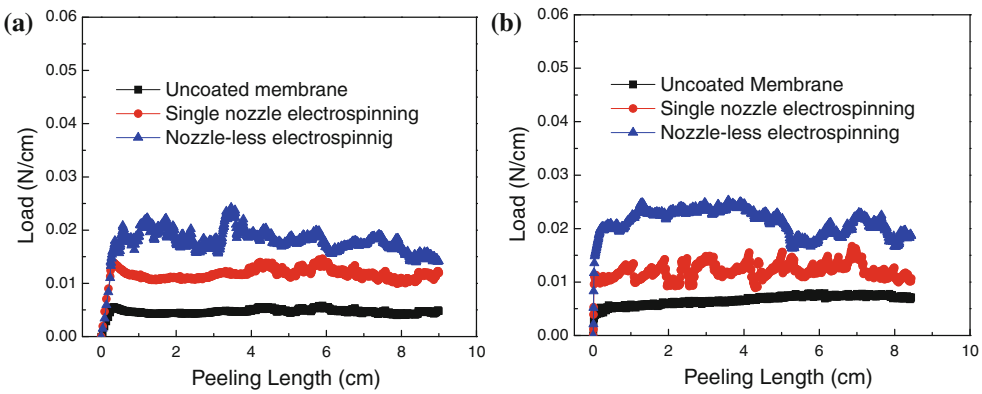

Fig. 10 Peeling load as a function of length for peeling **a** PVDF and **b** PVDF-*co*-CTFE nanofiber-coated PP membranes from the battery electrode. For comparison, uncoated membrane is also shown

and PVDF-*co*-CTFE nanofiber-coated membranes from the battery electrode. For comparison, the results for peeling the uncoated membrane from the battery electrode are also shown. The adhesion of the uncoated membrane to the battery electrode is low. However, the PVDF and PVDF-*co*-CTFE nanofiber coatings improve the adhesion between the separator and the electrode. Electrospun nanofibers in membrane/electrode assemblies contribute to enhanced adhesion because they provide a fibrous polymer network which can bind the PP membrane substrate to the battery electrode during lamination.

As shown in Fig. 10, the PVDF and PVDF-*co*-CTFE nanofiber-coated PP membrane separators produced by nozzle-less electrospinning have better adhesion to the electrode than those prepared by the single nozzle electrospinning method. The smaller diameters of the fibers making up the nozzle-less electrospun nanofiber coating resulted in a larger contact area of the fibers to the surface of the electrode which may be contributing to enhanced adhesion.

To further demonstrate the improved adhesion between nanofiber-coated membrane and the electrode, SEM images

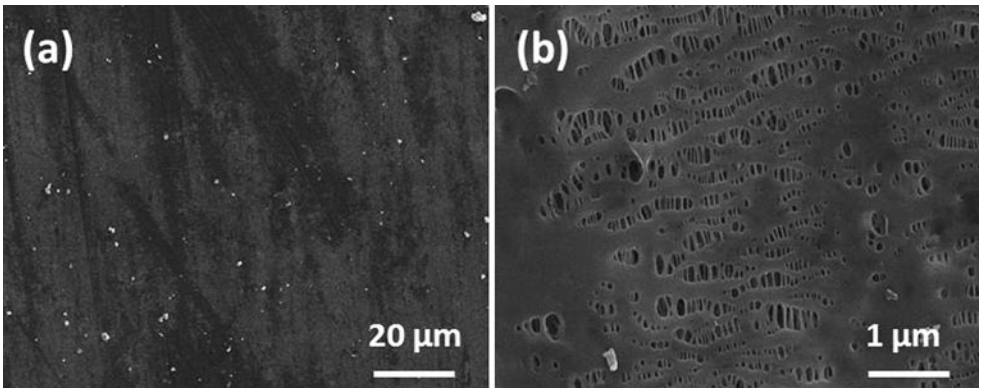

Fig. 11 SEM images of uncoated membrane after being peeled off from the electrode. Magnification: 1000× (**a**), 20,000× (**b**)

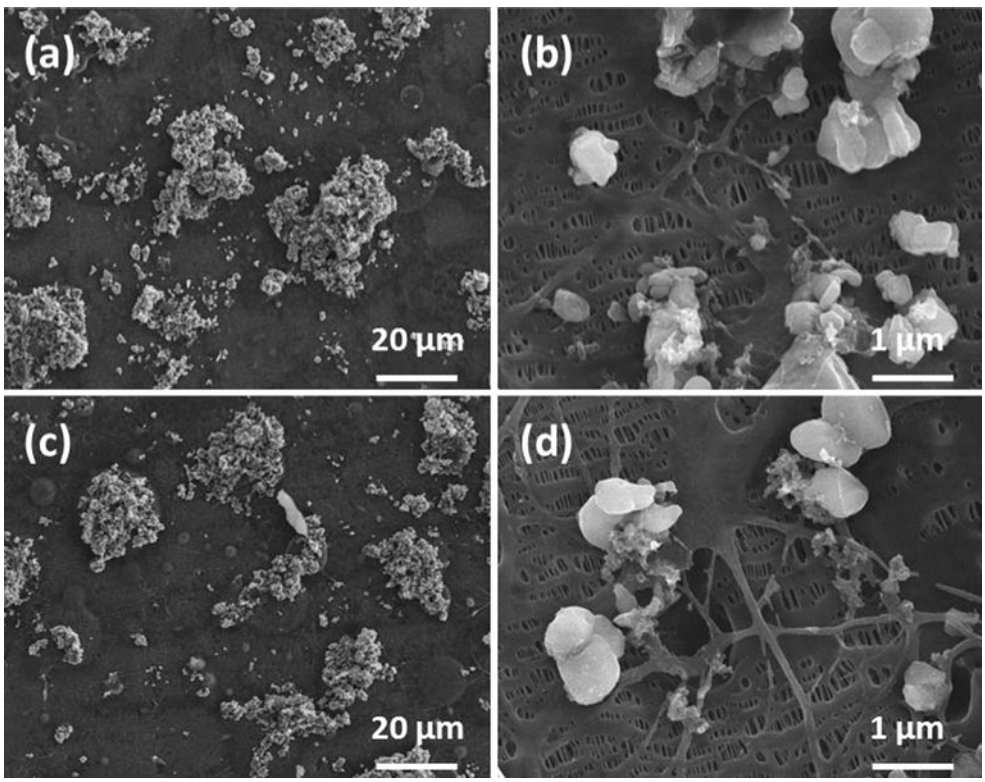

Fig. 12 SEM images **a**, **b** PVDF, and **c**, **d** PVDF-*co*-CTFE nanofiber-coated membranes after being peeled off from the electrode. Nanofiber coatings were prepared by single nozzle electrospinning. Magnification: 1000× (**a**, **c**), 20,000× (**b**, **d**)

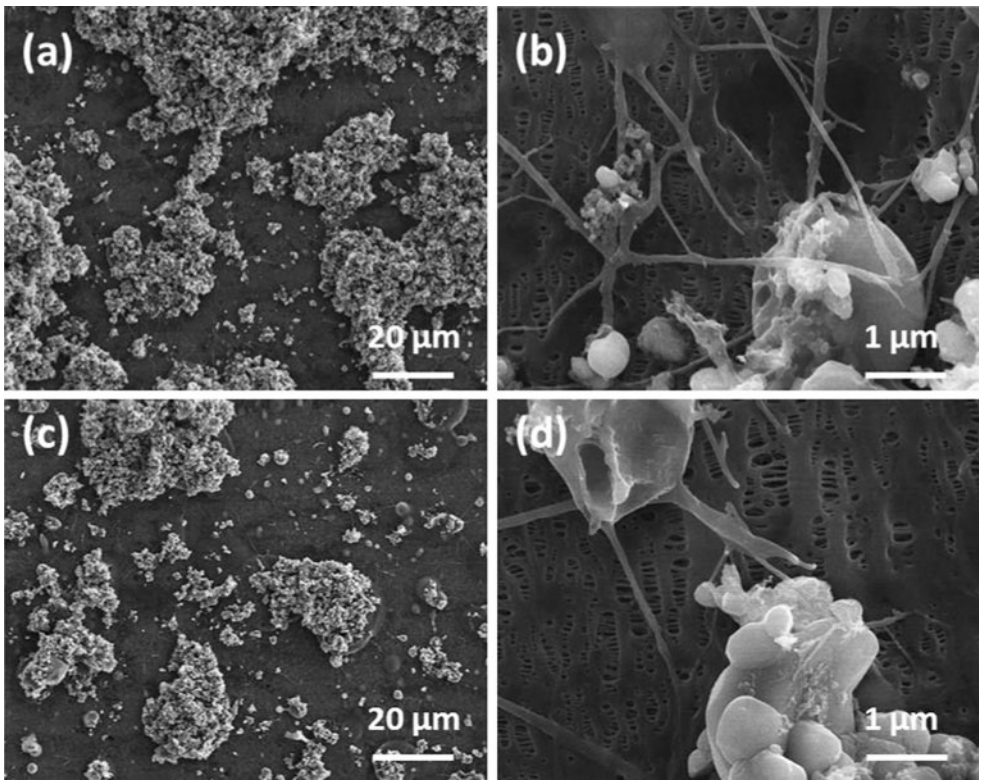

Fig. 13 SEM images of **a**, **b** PVDF and **c**, **d** PVDF-*co*-CTFE nanofiber-coated membranes after being peeled off form the electrode surface. Nanofiber coatings were prepared by nozzle-less electrospinning. Magnification: 1000× (**a**, **c**), 20,000× (**b**, **d**)

were taken on the membranes after they were peeled off from the electrode surface. Figure 11 shows SEM images of the uncoated membrane after the peel test. It is seen that the uncoated membrane is clear and only a few small cathode particles were removed from the electrode surface and were left on the membrane, indicating insufficient adhesion between the uncoated membrane and the electrode. Figures 12 and 13 show the SEM images of PVDF and PVDF-*co*-CTFE nanofiber-coated membranes after the peel tests. The SEM micrographs show the presence of cathode particles adhered to the PVDF nanofibers indicating that the electrospun nanofiber coating adhered both to the PP membrane substrate and to the surface of the electrode. This confirms that the nanofiber coating can significantly improve the adhesion of the separator membrane to the electrode.

Summary

PVDF and PVDF-*co*-CTFE nanofiber-coated Celgard® 2400 PP membrane separators were prepared by single nozzle and nozzle-less electrospinning methods. Compared with single nozzle electrospinning, the nozzle-less electrospinning produced nanofibers with smaller diameters and better adhesion to the membrane substrate. The electrolyte uptake capacities and separator-electrode adhesion of nanofiber-coated PP membranes were evaluated. The nanofiber-coated membranes exhibited higher electrolyte uptake capacities and stronger separator-electrode adhesion than uncoated membranes. Among the polymer nanofiber coatings evaluated, the PVDF-*co*-CTFE nanofiber-coated Celgard® PP microporous membrane separators prepared by nozzle-less electrospinning presented the highest electrolyte uptake capacity and the strongest separator-electrode adhesion.

Acknowledgements This work was financially supported by Department of Energy (EE0002611-600). The authors acknowledge Gerald Rumierz, Lie Shi, Prem Ramadass, and Bill Paulus at Celgard LLC for their kind assistance. The authors also thank Solvay Inc. and Kureha Corp. for providing PVDF and PVDF-*co*-CTFE samples.

References

1. Zhang X, Ji L, Toprakci O, Liang Y, Alcoutlabi M (2011) Polym Rev 51:239
2. Goodenough JB, Kim Y (2011) J Power Sources 196:6688
3. Jeong G, Kim YU, Kim H, Kim YJ, Sohn HJ (2011) Energy Environ Sci 4:1986
4. Arora P, Zhang Z (2004) Chem Rev 104:4419
5. Ji L, Lin Z, Alcoutlabi M, Zhang X (2011) Energy Environ Sci 4:2682
6. Zhang SS (2007) J Power Sources 164:351
7. Stephan AM (2006) Eur Polym J 42:21
8. Park JH, Cho JH, Park W, Ryoo D, Yoon SJ, Kim JH, Jeong YU, Lee SY (2010) J Power Sources 195:8306
9. Janmey RM (2007) US Patent 6828061, 7 Dec 2007

10. Arrance FC (1970) US Patent 3542596, 24 Nov 1970
11. Shinohara Y, Tsujimoto Y, Nakano T (2002) US Patent 6447958, 10 Sept 2002
12. Pekala RW, Khavari M (2002) US Patent 20020001753, 3 Jan 2002
13. Hashimoto T, Totsuka H, Takahata M, Takanashi M, Oota Y, Sano K (2010) US Patent 20100316912, 16 Dec 2010
14. Carlson SA (2004) US Patent 20040185335, 23 Sept 2004
15. Ying Q, Carlson SA, Skotheim TA (2001) US Patent 6194098, 27 Feb 2001
16. Lang CD, Faircloth TJ (2011) US Patent 20110086164, 14 April 2011
17. Rice WC, Puglia JP (2003) US Patent 6536605, 25 March 2003
18. Kim JH, Yu JS, Choi JH (2011) US Patent 8003263, 23 Aug 2011
19. Choi HS, Lee YK, Park CH, Choi BY, Lee KJ (2010) US Patent 20100055401, 4 March 2010
20. Shiraishi M, Someya K (2003) US patent 6666165, 23 Dec 2003
21. Marston JO, Simmons MJH, Decent SP (2007) Exp Fluids 42:483
22. Jung HR, Ju DH, Lee WJ, Zhang X, Kotek R (2009) Electrochim Acta 54:3630
23. Raghavan P, Manuel J, Zhao X, Kim DS, Ahn JH, Nah C (2011) J Power Sources 196:6742
24. Liang Y, Ji L, Guo B, Lin Z, Yao Y, Li Y, Alcoutlabi M, Qiu Y, Zhang X (2011) J Power Sources 196:436
25. Carol P, Ramakrishnan P, John B, Cheruvally G (2011) J Power Sources 196:10156
26. Lee SW, Choi SW, Jo SM, Chin BD, Kim DY, Lee KY (2006) J Power Sources 163:41
27. Choi SS, Lee YS, Joo CW, Lee SG, Park JK, Han KS (2004) Electrochim Acta 50:339
28. Yang C, Jia Z, Guan Z, Wang L (2009) J Power Sources 189:716
29. Gao K, Hu X, Dai C, Yi T (2006) Mater Sci Eng B 131:100
30. Kim JR, Choi SW, Jo SM, Lee WS, Kim BC (2004) Electrochim Acta 50:69
31. Choi SW, Jo SM, Lee WS, Kim YR (2003) Adv Mater 15:2027
32. Kim JR, Choi SW, Jo SM, Lee WS, Kim BC (2005) J Electrochem Soc 152:A295
33. Raghavan P, Zhao X, Manuel J, Chauhan GS, Ahn JH, Ryu HS, Ahn HJ, Kim KW, Nah C (2010) Electrochim Acta 55:1347
34. Cheruvally G, Kim JK, Choi JW, Ahn JH, Shin YJ, Manuel J, Raghavan P, Kim KW, Ahn HJ, Choi DS, Song CE (2007) J Power Sources 172:863
35. Ding Y, Zhang P, Long Z, Jiang Y, Xu F, Di W (2009) J Membr Sci 329:56
36. Djian D, Alloin F, Martinet S, Lignier H, Sanchez JY (2007) J Power Sources 172:416
37. Dong Z, Kennedy SJ, Wu Y (2011) J Power Sources 196:4886
38. Kim JY, Lim DY (2010) Energies 3:866
39. Burger C, Hsiao BS, Chu B (2006) Annu Rev Mater Res 36:333
40. Lyons J, Ko F (2005) Polym News 30:1
41. Baumgarten PK (1971) J Colloid Interface Sci 36:71
42. Subbiah T, Bhat GS, Tock RW, Parameswaran S, Ramkumar SS (2005) J Appl Polym Sci 96:557
43. Deitzel JM, Kleinmeyer J, Harris D, Beck Tan NC (2001) Polymer 42:261
44. Song MK, Kim YT, Kim YT, Cho BW, Popov BN, Rhee HW (2003) J Electrochem Soc 150:A439
45. Dias FB, Plomp L, Veldhuis JBJ (2000) J Power Sources 88:169